The Company of Biologists

RESEARCH ARTICLE

Monopolatic motion vision in the butterfly *Papilio xuthus*

Finlay J. Stewart, Michiyo Kinoshita and Kentaro Arikawa*

ABSTRACT

The swallowtail butterfly *Papilio xuthus* can perceive the linear polarization of light. Using a novel polarization projection system, we recently demonstrated that *P. xuthus* can detect visual motion based on polarization contrast. In the present study, we attempt to infer via behavioural experiments the mechanism underlying this polarization-based motion vision. *Papilio xuthus* do not perceive contrast between unpolarized and diagonally polarized light, implying that they cannot unambiguously estimate angle and degree of polarization, at least as far as motion detection is concerned. Furthermore, they conflate brightness and polarization cues, such that bright vertically polarized light resembles dim unpolarized light. These observations are consistent with a one-channel 'monopolatic' detector mechanism. We extend our existing model of motion vision in *P. xuthus* to incorporate these polarization findings, and conclude that the photoreceptors likely to form the basis for the putative monopolatic polarization detector are R3 and R4, which respond maximally to horizontally polarized green light. R5–R8, we propose, form a polarization-insensitive secondary channel tuned to longer wavelengths of light. Consistent with this account, we see greater sensitivity to polarization for green-light stimuli than for subjectively equiluminant red ones. Somewhat counter-intuitively, our model predicts greatest sensitivity to vertically polarized light; owing to the non-linearity of photoreceptor responses, light polarized to an angle orthogonal to a monopolatic detector's orientation offers the greatest contrast with unpolarized light.

INTRODUCTION

Despite having vastly inferior spatial acuity to humans, many insects could be said to have a richer visual experience than we do. For instance, the Japanese yellow swallowtail butterfly (*Papilio xuthus*) not only has tetrachromatic colour vision, but can also perceive the polarization of light (Kinoshita and Arikawa, 2014). This refers to the orientation in which light waves oscillate, and in the case of linear (or plane) polarization, can be fully specified by three parameters: intensity, angle of polarization (AoP) and degree of linear polarization (DoLP). Intensity simply refers to the photon count of the light. AoP is the predominant orientation among the waves that constitute the light, and has a period of 180 deg. DoLP describes what proportion of the waves are aligned with the AoP, and ranges from 0 (unpolarized, i.e. all orientations are equally

Department of Evolutionary Studies of Biosystems, SOKENDAI (The Graduate University for Advanced Studies), Shonan International Village, Hayama, Kanagawa, 240-0193 Japan.

*Author for correspondence (arikawa@soken.ac.jp)

K.A., 0000-0002-4365-0762

abundant and thus the AoP is undefined) to 1 (fully polarized) (Foster et al., 2018).

The rich visual sensation of *P. xuthus* is a product of its elaborate retinal organization, featuring eight spectrally distinct classes of photoreceptor (Koshitaka et al., 2008). Each ommatidium of the eye contains nine photoreceptors, organized in one of three randomly distributed configurations, which are referred to as ommatidial types (Table 1). The photoreceptors in the R1 and R2 positions are short-wavelength-sensitive (UV, violet or blue, depending on ommatidial type), and have vertically oriented microvilli, meaning that they respond maximally to vertically polarized (V-pol) light, at least around the equator of the eye (Arikawa and Uchiyama, 1996). R3 and R4 are green-sensitive throughout the retina and are tuned to horizontally polarized (H-pol) light. R5–R8 are long-wavelength-sensitive (red, broad-band or green) and sensitive to diagonal polarization angles, forming two mutually roughly orthogonal pairs. Little is known about the diminutive R9, but it is also thought to be long-wavelength-sensitive. Although *P. xuthus* exhibit some subtle differences between the dorsal and ventral regions of the eye in terms of pigments expressed (Kitamoto et al., 1998; Arikawa et al., 1999), these are less pronounced than those found in many other butterfly species (Stavenga et al., 2001; Awata et al., 2009, 2010).

The organization outlined above prompts a question: if photoreceptors with different polarization tunings also have different spectral sensitivities, how can *Papilio* butterflies disentangle polarization, colour and brightness signals? The answer seems to be that they do not. In ovipositing *Papilio aegus*, polarization alters colour perception (Kelber, 1999; Kelber et al., 2001), whereas foraging *Papilio xuthus* respond to equiluminant but differently polarized lights as though they vary in brightness (Kinoshita et al., 2011). These two accounts are not mutually exclusive; it may well be the case that both species conflate polarization with both intensity and colour information, but the salience of these cues depends on the behavioural context. Indeed, no invertebrate so far studied is able to unambiguously detect the e-vector of light as an independent visual modality (Labhart, 2016).

In the present study, we investigated the role of polarization in motion vision, which is presumably distinct from the 'object vision' employed by the animals in the oviposition and foraging contexts mentioned above. Using a novel projection system, we recently demonstrated that *P. xuthus* could detect motion using polarization contrast (Stewart et al., 2017). However, they were unresponsive to a moving diagonally polarized object against an unpolarized (un-pol) background, despite having the sensory hardware (R5–R8) to potentially detect diagonal polarization. We also identified an anisotropy, whereby they were more sensitive to V-pol objects than to H-pol ones of the same DoLP.

The aim of this study was to explain these phenomena in terms of the photoreceptors and early neural circuits involved in motion detection. We previously investigated the motion vision of *P. xuthus* with regard to colour vision (Stewart et al., 2015), and found that unlike flies and bees, which have achromatic motion vision (Kaiser and Liske, 1974; Yamaguchi et al., 2008), *P. xuthus* can detect

List of symbols and abbreviations

AoP   angle of polarization
DoLP   degree of linear polarization
H-pol   horizontally polarized
R1,2,3…   photoreceptor 1, 2, 3…
un-pol   unpolarized
V-pol   vertically polarized
$\Delta\phi$ difference in pitch orientation of the head between the onset and offset of the stimulus, i.e. the behavioural metric we use as a proxy for motion detection

motion based on chromatic contrast. This implies that a spectrally diverse set of photoreceptors must contribute to motion vision, and based on our modelling, we concluded that the photoreceptors in question are primarily the green-sensitive R3/4, along with a small contribution from the red-, broad-band- or green-sensitive R5–R8 (Stewart et al., 2015). We proposed a two-channel model in which ON and OFF contrasts are processed separately. Such an architecture has been well documented in flies (Joesch et al., 2010), and indeed a similar parallel processing scheme is found in the mammalian retina (Wässle, 2004). Remarkably, we observed an interaction in the sensitivity of *P. xuthus* to a moving edge between its polarity (i.e. ON or OFF) and its colour. Therefore, we posited that the two motion processing channels of *P. xuthus* take input from spectrally dissimilar populations of photoreceptors, and thus have different spectral tunings: the ON channel takes more input from R5–R8, whereas the OFF channel is more dominated by R3/4.

A natural question is whether this existing model can be extended to account for polarization. For R3/4, this is straightforward: both of these photoreceptors respond maximally to H-pol light. R5–R8 present more of a puzzle as they are sensitive to diagonal AoPs, forming two roughly orthogonal pairs. Because of the behavioural insensitivity of *P. xuthus* to diagonal polarization (Stewart et al., 2017), we hypothesize that the responses of R5–R8 are pooled, largely eliminating their polarization sensitivity. Thus, we propose that the polarization detection mechanism is monopolatic, i.e. containing just one polarization-sensitive channel, namely the H-pol-sensitive R3/4.

We can generate some qualitative predictions from this extended model, which we test behaviourally in this study. First, a fixed (i.e. not rotating) monopolatic detector cannot disambiguate intensity and AoP (Bernard and Wehner, 1977; How and Marshall, 2014; Labhart, 2016). Therefore, dim H-pol, moderate un-pol and bright V-pol light should be perceptually similar. Second, if the

long-wavelength-sensitive R5–R8 make little or no contribution to polarization detection, sensitivity to polarization contrast should be lower for red light than for green light. Until recently, it would have been technically infeasible to test these predictions experimentally, because of the difficulty of presenting moving images containing both intensity and polarization contrast. Fortunately, however, this is relatively straightforward with our polarization projection system.

MATERIALS AND METHODS
Apparatus
The polarization projection system was described in detail in Stewart et al. (2017). A digital light processing (DLP) projector (Texas Instruments LightCrafter 4500) rear-projected through a spinning linear polarizer onto a polarization-preserving screen (Da-Lite 3D Virtual Black). The polarizer was mounted on a brushless DC motor, and its rotation was synchronized with the frame rate of the projector, such that it completed half of a rotation for each video frame. Each frame was split into four sequentially presented subframes corresponding to different angles of polarization. By presenting different images in these four 'polarization channels', AoP and DoLP could be manipulated on a pixel-by-pixel basis, in much the same way as hue and saturation are produced by mixing colour channels. The video was monochrome for all experiments (other than the preliminary experiment to find the subjective equiluminance point of green and red; see below), i.e. the spectral content of the light (supplied from the LED light engine) was constant between all subframes. Unless otherwise stated, cyan light (blue and green LEDs on simultaneously) was used.

The projector resolution was 912×1140 pixels in a diagonally oriented grid (the aspect ratio was 16:10 widescreen). The graphics card (Nvidia GeForce GTX 670) was set to output video at 56 Hz, but the display system operated at twice this rate (112 Hz), drawing each frame twice. As the gain of the fastest photoreceptors of *P. xuthus* is <0.15 at 100 Hz (Kawasaki et al., 2015), the animals should perceive minimal flickering in the image. Thus, each subframe had a duration of $(112 \times 4)^{-1}$=2232 µs. The intensity of each subframe pixel was controlled using pulse width modulation with 5-bit precision.

The projection system cannot perfectly control intensity, AoP and DoLP completely independently; altering one of these parameters can introduce unwanted residual contrast in the other modalities. These effects are characterized in Stewart et al. (2017); of particular relevance to the present study is the observation that highly polarized light is attenuated in intensity by ~5% compared with supposedly equiluminant un-pol light (Stewart et al., 2017, their fig. 2B). Unless otherwise stated, we refer to 'nominal' values for these parameters, i.e. those expected under the unrealistic assumption of ideal operation, so it should be borne in mind that the given values are approximations.

Animals
Laboratory-reared spring-form adult Japanese yellow swallowtail butterflies (*Papilio xuthus* Linnaeus 1767) of both sexes were used for all experiments.

Experimental protocol
In this study, we employed a directly analogous approach to the one we previously used to investigate chromatic motion vision (Stewart et al., 2015). A butterfly was suspended by its wings with its head approximately 11 cm from the centre of the screen, on which the image measured approximately 20×12 cm (horizontal×vertical), i.e.

Table 1. Retinal organization of Papilio xuthus

Photoreceptor	Mv orientation (deg)	Spectral tuning (varies according to ommatidium type)		
		Type I	Type II	Type III
R1, R2	0 (V)	UV/blue*	Violet	Blue
R3, R4	90 (H)	Green	Green	Green
R5, R7	35	Red	Broad-band	Green
R6, R8	145			
R9	0	Red?	Broad-band?	Green?

*Type I R1/2 comprise exactly one UV-sensitive and one blue-sensitive photoreceptor.
The orientation of the microvilli (Mv) corresponds to the AoP to which the photoreceptor responds maximally. Shaded rows indicate the photoreceptors thought to be involved in motion vision; R3/4 are heavily shaded to indicate their dominant role in this visual modality (Stewart et al., 2015). Adapted from Kinoshita and Arikawa (2014).

subtending a visual angle of ∼85×53 deg in the frontal visual field. At the centre of the screen, each pixel subtended a (diagonally oriented) square of ∼0.3 deg. A camera was positioned to the side of the butterfly to record its responses. It should be noted that because of viewing angle effects, the edges of the screen would appear substantially darker to the butterfly than the centre. These dim edge regions also contain some polarization artefacts (Stewart et al., 2017, their fig. 2C–H).

Because of the aforementioned issue of unavoidable residual contrast, we performed control experiments where the animal was rotated 90 deg with respect to the screen. In this way, we could confirm that any effects of AoP could indeed be attributed to the apparent AoP from the animal's perspective, rather than any artefact of the display system. For these 'rotated' control experiments, the animal was positioned such that its dorso-ventral axis was parallel with the horizon, and it was filmed via a mirror placed underneath it. Thus, vertical polarization would appear horizontal to the animal, and vice versa. The animals made little or no attempt to rotate their heads to an upright orientation.

Stimuli were generated using a custom-written Java program. Each stimulus consisted of an object and background differing in their intensity and/or polarization properties. For each stimulus, the object swept upwards over the screen, taking 2 s to cover its entire vertical extent. Batches of up to nine stimuli were presented sequentially, separated by intervals of 15 s. Within each experiment, the order of batches was randomized.

In the case of 'stripe' stimuli, the object was a horizontal bar covering the entire width of the image and one-eighth of its height (∼7 deg angular subtense). The situation was similar in 'single edge' conditions, except that the object lacked a trailing edge, and thus filled up the whole screen by the time of its offset. In the rotated control, the stimulus pattern was rotated and stretched to meet the new aspect ratio, i.e. the object moved faster in absolute terms and the bar was wider (∼11 deg).

In the intensity/polarization experiment, a stripe with a nominal DoLP of 0.39 (0.66 in the rotated control, to compensate for the animal's lower overall responsiveness) and an AoP of either 0 or 90 deg (vertical and horizontal, respectively) was presented on an un-pol background of variable intensity, in randomized order. In all other experiments, the stimuli were presented in order of increasing contrast, to minimize habituation effects. For the orthogonal polarization experiment, the background and stripe had equal (variable) DoLP, but AoPs separated by 90 deg. Finally, in the edge polarity experiment, a single edge stimulus was used. In the advancing polarization case, a polarized object (of variable DoLP) expanded over an un-pol background; the reverse was the case for receding polarization.

Analysis

Images of the butterfly were captured immediately prior to the stimulus onset and at its offset 2 s later. From these, we estimated the head pitch by measuring the angle of the antennae. This was done in ImageJ by thresholding the images, defining a region of interest covering the shafts of the antennae, and fitting ellipses to the two resulting shapes. The difference in the angles before and after the stimulus, averaged over the two antennae, was taken as the behavioural metric $\Delta\phi$. Positive $\Delta\phi$ values correspond to the direction of the stimulus motion, i.e. dorsal. To estimate the background intensity z at which responses were minimal in the intensity/polarization experiment, we fitted a parabola of the form:

$$\Delta\phi = g(\text{background intensity} - z)^2, \qquad (1)$$

to each individual's response curve, where g is a gain parameter that we subsequently ignore. For polarization sensitivity experiments, we fitted sigmoidal functions of the form:

$$\sqrt{\Delta\phi} = \frac{g}{1 + \exp(\text{slope}(\text{offset} - \text{DoLP}))}, \qquad (2)$$

and from this interpolated the threshold DoLP at which a criterion level ($\sqrt{\Delta\phi}=0.5$, i.e. $\Delta\phi=0.25$ deg) was reached. (The square root is taken to reduce the influence of large suprathreshold antennal moves on the sigmoid fit; negative $\Delta\phi$ values are set to 0.) If the criterion level was never reached (i.e. if $g<0.5$), we set the threshold to an arbitrary high value. Thus, only non-parametric statistical procedures can be applied to this data. All non-linear function fitting was performed using the nlsLM package for R.

Obtaining subjectively equiluminant green and red light

We reconfigured the display system to make the polarizer spin asynchronously with the projector, thereby scrambling the polarization contrast such that it was not coherent from one frame to the next. In addition, we set the green and red LEDs to alternate between subframes, allowing us to present a red stripe against a green background. The overall brightness of the LEDs can be modulated by adjusting the current supplied to them, via an 8-bit setting in the projector configuration. We set the red LED to a saturated level (setting 135), and then adjusted the green LED current setting until minimal responses were observed. At this point we assumed that negligible intensity contrast existed, and motion was detected based on chromatic contrast alone (Stewart et al., 2015). We settled on a green current setting of 11. Fig. S1 shows the results of using these current settings and programmatically varying the intensity of the red stripe, in a similar fashion to the intensity/polarization experiment. By fitting parabolas to these curves (see above), we estimated that the subjective luminance of the green light was 98.0±2.4% of that of the red (mean±s.e.m., $n=12$).

Modelling

In the present study, we extend the model of motion detection that we developed to investigate the role of chromatic contrast in motion detection, as described in Stewart et al. (2015). For the purposes of the present study, we are not concerned with colour contrast, and thus ignore spectral sensitivity. The architecture of the model is summarized in Fig. 1. We model the relative activation a of a given photoreceptor group p (i.e. R3/4 or R5–R8) to polarized light as follows:

$$a_p(d, \theta) = (1 - d) + d\left(1 + \cos(2(\theta - \theta_p))\frac{(s_p - 1)}{(s_p + 1)}\right), \qquad (3)$$

where s_p and θ_p are the polarization sensitivity ratio and angular tuning, respectively, of photoreceptor group p, and d and θ are the DoLP and AoP, respectively, of the light. For R3/4, $\theta_p=90$ deg (horizontal) and $s_p=2$. The latter parameter is based on the theoretical value assuming perfectly cylindrical microvilli and no additional sensitivity-enhancing mechanisms such as inter-photoreceptor opponency. This estimate is in line with electrophysiological data; for R3/4 in type II ommatidia, for instance, $s_p=1.93\pm0.11$ (Bandai et al., 1992). We assume the responses of R5–R8 are pooled, cancelling out their individual polarization sensitivities such that their s_p collectively is 0 (and thus their θ_p undefined).
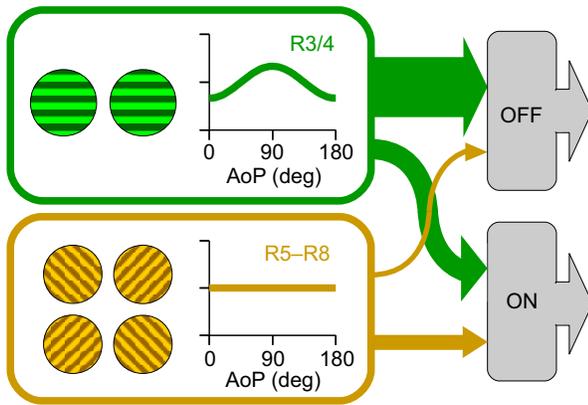
Fig. 1. Model overview. The motion detection model takes input from two groups of photoreceptors: the green-sensitive R3/4, which respond maximally to horizontal polarization (H-pol); and the red-, broad-band- or green-sensitive (depending on ommatidial type) R5–R8. Though R5–R8 are individually sensitive to polarization, we assume that collectively they are not, as their tunings cancel each other. The photoreceptors feed into two parallel motion-sensitive channels: one detecting ON polarity moving edges, and one OFF. The widths of the arrows indicate the weightings of their contributions. The ON channel takes a greater proportion of its input from R5–R8 than the OFF channel. AoP, angle of polarization.

The relative activation a_p is passed into the Naka–Rushton model (Naka and Rushton, 1966a,b) to obtain the output of the photoreceptor:

$$o_p(I,d,\theta) = \frac{(Ia_p(d,\theta))^n}{(Ia_p(d,\theta))^n + K^n},\qquad(4)$$

where I is the intensity of the light, and K (=1.5) and n (=0.7) define the offset and slope of the log-sigmoidal function, respectively. To approximate the intensity artefact produced by the projector (see 'Apparatus', above), we assume that I is 0.95 for polarized and 1.0 for un-pol light by default.

The contrast c between two image regions, which we can conceptualize as figure (f) and background (b), is the squared difference between the outputs of the photoreceptor group (p) in

question:

$$c_p = (o_p(I_f,d_f,\theta_f) - o_p(I_b,d_b,\theta_b))^2.\qquad(5)$$

(The squaring implicitly represents the multiplicative interaction between the two channels of the classical 'delay and correlate' model of motion detection.) As in the original model, we hypothesize that the two pathways (R3/4 and R5–R8) are specialized for detecting OFF and ON moving contrasts, respectively. Accordingly, $c_{3/4}$ is attenuated by dividing by parameter α (=3.0) if the contrast polarity is positive, and c_{5-8} is divided by α if it is negative. This step is omitted for stripe-type stimuli, as they have one edge of each polarity.

Finally, the signals from the two pathways are combined according to weighting parameter β (=0.2), and passed through a logarithmic function to yield the output of the model as whole:

$$\text{output} = \log((1-\beta)c_{R3/4} + \beta c_{R5-8} + \varepsilon) - \log(\varepsilon),\qquad(6)$$

where ε is a small constant (=0.001) included merely to prevent errors when the contrast is zero. An implementation of the model, along with the behavioral data upon which it is based, can be found in Dataset 1.

RESULTS
Polarization is perceived as false intensity

To investigate the relationship between polarization and intensity contrast, we presented a rising polarized stripe against an un-pol background (Fig. 2A). We varied the intensity of the background while holding the intensity and polarization properties of the stripe constant. Results are shown in Fig. 2B. For both the H-pol and V-pol objects, the response dipped to a level not significantly different from zero for certain background intensities. By fitting parabolas to individual responses, we can estimate the relative intensity at which the contrast between background and stripe was minimal (Fig. 2C). For a V-pol stripe, the median equiluminance point was 0.89, versus 0.97 for H-pol. This difference is significant (paired Wilcoxon test: $P<0.001$, $n=15$), indicating that V-pol light is perceived to be darker than H-pol light, in the context of motion vision.
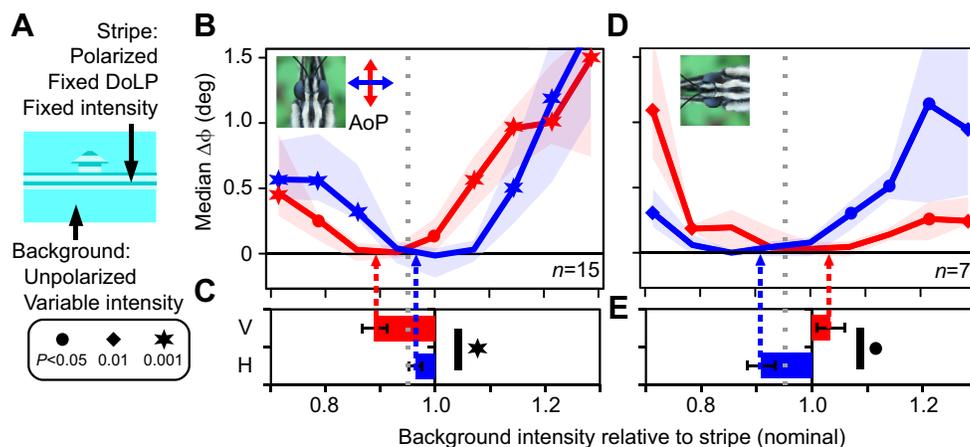
Fig. 2. Polarization/intensity experiment. (A) Schematic diagram of stimuli. (B) Behavioural response to vertically polarized (V-pol; red) and H-pol (blue) stripes against an unpolarized (un-pol) background of variable intensity. Shaded regions are interquartile ranges; symbols denote probability of value being ≤0 (one-tailed, one-sample Wilcoxon test). The x-axis refers to nominal intensity; owing to an artefact of the projector (see Materials and Methods), we estimate that the stripe and background are truly equiluminant at ~0.95, indicated by the dotted grey line. Sample sizes (n) refer to numbers of individuals. DoLP, degree of linear polarization. (C) Mean estimates of subjective equiluminance point, obtained by fitting parabolas to each individual's responses. These differ significantly between V- and H-pol (Wilcoxon test). Error bars are ±1 s.e.m. (D,E) As B,C, but for the rotated control condition, where the animal is oriented sideways and a vertical stripe sweeps horizontally across the screen. Thus, V-pol light on the screen is H-pol from the butterfly's perspective and vice versa.

On its own, this finding could be attributed to artefacts of the display system. To exclude this possibility, we repeated the experiment with the animal rotated 90 deg about its roll axis, such that horizontal polarization would appear vertical, and vice versa (Fig. 2D,E). We now see the opposite effect, with the equiluminance point lower for H-pol than V-pol (0.91 versus 1.03, $P=0.016$, $n=7$), reinforcing the view that V-pol is indeed subjectively darker.

Modelling results

Our model posits that the R3/4 photoreceptors play a dominant role in motion detection, but that R5–R8 also contribute as a secondary channel. We assume that the responses of R5–R8 are pooled within a given ommatidium, cancelling out their individual polarization sensitivities. The model is therefore monopolatic, containing just one polarization-sensitive channel – R3/4 – which responds maximally to H-pol light (Fig. 1).

Fig. 3A shows the response of the model to the stimuli used in our previous polarization study (Stewart et al., 2017), i.e. a moving stripe of various AoPs against an un-pol background. The model qualitatively reproduces the experimental findings: sensitivity is greatest to a V-pol object, it is lower for an H-pol one, and essentially zero for diagonal polarization. The bias towards V-pol can be attributed in part to the projector intensity artefact: the stripe is objectively darker than the background, which boosts the subjective brightness decrement for V-pol but attenuates the subjective increment for H-pol. However, this does not fully explain the asymmetry. When we model a truly equiluminant situation, greater responses are still elicited by a V-pol stripe (Fig. 3B) because of the non-linearity of photoreceptor responses (see Discussion).

Fig. 3C shows the results of modelling the polarization/intensity experiment of the previous section. Again, the results qualitatively match the behavioural data. Interestingly, the curves' minima are above zero, implying that although polarization is conflated with intensity, contrasts in the two modalities cannot perfectly cancel each other out. The minimum response for a V-pol stripe is higher than that for H-pol (0.045 versus 0.035), again indicating that V-pol offers greater subjective contrast with un-pol than does H-pol.

A key feature of our model is that it posits that the two groups of photoreceptors (R3/4 and R5–R8) contribute unevenly to detecting ON- and OFF-polarity edges. Specifically, OFF-edge detection receives disproportionate input from the polarization-sensitive R3/4. Therefore, the model predicts greater sensitivity to a V-pol region advancing into an un-pol region than vice versa. Conversely, we would predict greater sensitivity to a receding H-pol edge than an advancing one (Fig. 4A,B), though the sensitivity would be lower overall for the H-pol stimuli than the V-pol ones because of the asymmetries discussed above.

Single-edge polarity experiment

To test the model's predictions, we presented *P. xuthus* with single-edge stimuli, where a polarized region swept upwards to fill a previously unpolarized screen, or vice versa. Fig. 4C shows the results. As predicted, we observed maximal sensitivity to advancing V-pol, which, based on our previous findings, would be perceived as an OFF-polarity edge. The animals were least sensitive to advancing H-pol, which would appear as an ON-edge. For the two remaining conditions, where the biases towards V-pol stimuli and OFF-edges were put in opposition to each other, we observed intermediate sensitivity.

Greater sensitivity to polarization of green light than red

If the green-sensitive R3/4 are responsible for polarization-based motion detection, then we would expect to observe greater sensitivity to the polarization of green light than, for instance, red. However, the motion vision system is more sensitive to green than red light in general (Stewart et al., 2015). Therefore, to test this prediction, we had to first obtain subjectively equiluminant green and red light, which we did by presenting a red stripe against a green background and finding the relative intensity at which the behavioural response was minimal (see Materials and Methods; Fig. S1).

Because the subjectively equiluminant light was rather dim in absolute terms, we maximized polarization contrast by presenting a polarized stripe against an orthogonally polarized background. Unfortunately, this had the side effect of producing pronounced edge artefacts because of the temporal phase difference between the presentation of different polarization angles (Fig. S2). For this reason, we pooled results from V-on-H and H-on-V trials in order to cancel out the constructive and destructive effects of these artefacts. Average response curves are shown in Fig. 5A, while Fig. 5B summarizes our estimates of relative sensitivity. As predicted, *P. xuthus* were more sensitive to V/H polarization contrast in green light than in red light (paired Wilcoxon test: $P=0.027$, $n=10$).
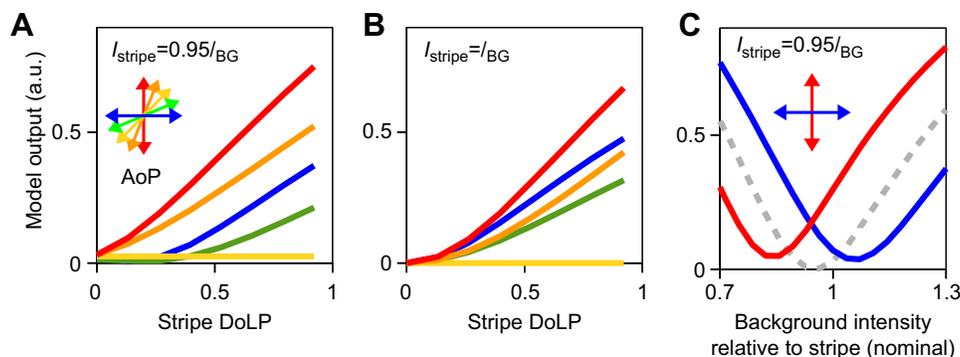
Fig. 3. Model results. (A) Modelled responses to a stripe of variable AoP (colours) and DoLP (*x*-axis) against an un-pol background. The stripe's intensity (I_{stripe}) is 95% that of the background (I_{BG}), approximating the projector artefact (see Materials and Methods) The model qualitatively reproduces the previous experimental findings that sensitivity to V-pol is greater than that to H-pol, and that sensitivity to diagonal polarization is negligible (Stewart et al., 2017: fig. 3). As diagonal polarization is indistinguishable from un-pol in this model, the small response seen for 45 deg AoP is caused by the brightness artefact. (B) As A, but assuming that the stripe and background are truly equiluminant, i.e. no artefact exists. The bias towards V-pol persists, albeit to a lesser extent. (C) Modelled responses for the polarization/intensity experiment shown in Fig. 2, taking the intensity artefact into consideration. The dashed grey line shows the response to a 95% intensity un-pol stripe, illustrating the effect expected owing to the artefact alone.
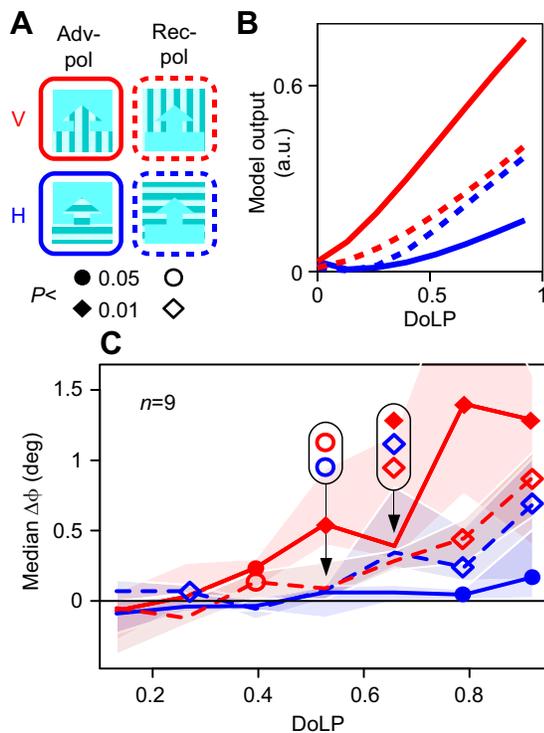
Fig. 4. Single-edge polarity experiment. (A) Schematic diagram of stimuli. A region of polarized light expands to fill a previously unpolarized screen, or vice versa. Adv-pol refers to the case where the polarized light advances to fill the screen; Rec-pol refers to the converse case, where the polarized region recedes. The two regions are objectively equiluminant. However, according to the results shown in Fig. 2, *Papilio xuthus* should subjectively perceive advancing H-pol (solid blue line) and receding V-pol (dashed red line) to be ON polarity edges (i.e. an advancing brightness increment), and the other two conditions (dashed blue, solid red) to be OFF polarity. (B) Model results for these stimuli. The intensity artefact is modelled: $I_{stripe}=0.95I_{BG}$. (C) Behavioural results. Shaded regions are interquartile ranges; symbols denote probability of value being ≤0 (one-tailed, one-sample Wilcoxon test). Solid symbols are for advancing polarization stimuli and open symbols for receding polarization. Where symbols would substantially overlap, they have been exploded for clarity (black rounded boxes). *n*=9 individuals.

Unsurprisingly, we observed little sensitivity to diagonally polarized stimuli. However, significant responses were elicited at high polarization degrees (Fig. 5A, open symbols). This could indicate some ability to perceive diagonal polarization, but we consider it more likely to be caused by imperfect alignment of the animal relative to the display and/or the aforementioned edge artefacts. We favour the latter explanation, as there is no significant difference in sensitivity to diagonal polarization contrast between green and red stimuli (*P*=0.36; Fig. 5B), suggesting that these responses are not based on polarization vision. For green stimuli, sensitivity is significantly greater to V/H contrast than to D/D (*P*=0.0039), but this is not the case for red stimuli (*P*=0.16), again reinforcing the view that green-sensitive photoreceptors are responsible for polarization detection.

DISCUSSION
Using a polarization projection system, we showed that *P. xuthus* butterflies' motion vision system perceives polarization as false brightness (Fig. 2): polarization contrast can be cancelled by intensity contrast (though perhaps not completely; see below). We implemented a monopolatic model (Fig. 1) closely based on our existing model of *P. xuthus* motion vision (Stewart et al., 2015).

This model represents the hypothesis that photoreceptors R3/4 constitute the sole polarization-sensitive channel involved in motion detection. Despite being originally devised based on chromatic contrast experiments, the model was able to qualitatively reproduce the polarization contrast effects we observed (Fig. 3). Furthermore, the model was able to predict how the polarity of single polarization contrast edges would affect their detectability (Fig. 4).

If polarization detection is based on the green-sensitive R3/4, one would expect that *P. xuthus* would be most sensitive to the polarization of green light (we did not explicitly model this, but – qualitatively at least – this is a clear prediction of our model). We confirmed that this is indeed the case: by first adjusting the relative intensity of (unpolarized) green and red light until minimal subjective contrast existed between them, we showed that *P. xuthus* were less sensitive to polarization contrast for red stimuli (Fig. 5). This observation provides new support to the argument we previously made (Stewart et al., 2015), that other photoreceptors besides R3/4 must contribute to motion vision. From the present study, we can deduce that these other photoreceptors are sensitive to longer wavelengths than R3/4 and have (collectively) lower polarization sensitivity; R5–R8 fit this description. Although we cannot exclude the possibility that the short-wavelength, V-pol sensitive R1/2 contribute in some way, in neither the previous study of chromatic contrast nor the present one was it necessary to include these photoreceptors in our model, implying that their role in motion detection is negligible.

The existence of two (or more) channels with different polarization tunings implies that polarization contrast cannot be perfectly cancelled by intensity contrast. This is because differently polarized light cannot appear equiluminant to both channels simultaneously. Therefore, we would predict that the responses in our intensity/polarization experiment (Fig. 2B,D) never actually drop to zero (Fig. 3C), in the same way that chromatic contrasts are always perceptible, independent of relative intensity (Stewart et al., 2015: Fig. 1C). However, the present study was insufficiently sensitive to detect these hypothesized residual responses.

Are R5–R8 really insensitive to polarization?
We have assumed for simplicity that the responses of R5–R8 are pooled, and therefore their individual polarization sensitivities cancel out, yielding a polarization-insensitive channel. However, this may be an oversimplification. In fact, R5/7 and R6/8 are not perfectly orthogonal; they respond maximally to AoPs of around 35 and 145 deg. Therefore, we would expect them collectively to respond maximally to V-pol, with a polarization sensitivity ratio of ~68% of their individual sensitivities.

It may therefore be the case that the motion detection system consists of two channels with orthogonal polarization tunings: H-pol sensitive R3/4 and V-pol sensitive R5–R8. Although this would superficially resemble a dipolatic detector, our model assumes that the responses of R3/4 and R5–R8 are combined additively, not subtractively. For this reason, no polarization opponency would exist. Instead, this would merely yield a monopolatic detector with slightly reduced sensitivity, as the polarization signal from R5–R8 would partially cancel that from R3/4. As our model is unable to make quantitative predictions of absolute sensitivity, we cannot exclude this possibility.
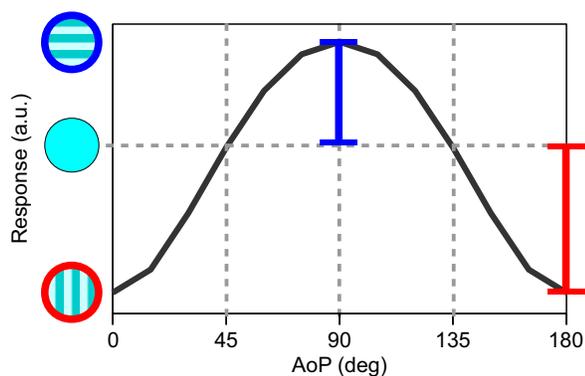
The asymmetry of monopolatic detectors
Our model predicts that V-pol objects elicit greater responses than equiluminant H-pol ones (Fig. 3B). To put it another way, V-pol light is more perceptually distinct from un-pol than is H-pol. It may
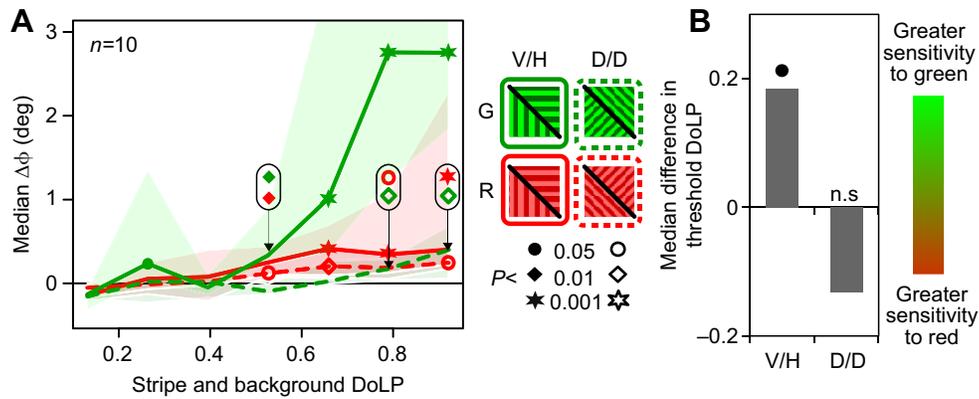
Fig. 5. Spectral polarization sensitivity. (A) Response curves for a polarized stripe on an equally but orthogonally polarized, objectively equiluminant background. Subjectively equiluminant green (G) and red (R) light was used (Fig S1). V/H refers to the averaged responses to a V-pol stripe on an H-pol background, and vice versa (see Fig. S2). D/D refers a 45 deg polarized stripe on a 135 deg polarized background. Shaded regions are interquartile ranges; symbols denote probability of value being ≤0 (one-tailed, one-sample Wilcoxon test). Solid symbols are for V/H and open symbols for D/D. Where symbols would substantially overlap, they have been exploded for clarity (black rounded boxes). n=10 individuals. (B) Sigmoidal functions were fitted to individual response curves to estimate the DoLP necessary to elicit a criterion response (see Materials and Methods), and these threshold values are compared for green and red light in a within-individual manner. Positive values indicate greater sensitivity for green, negative for red. Symbols denote P-values based on paired Wilcoxon tests.

therefore seem counter-intuitive for us to argue that the H-pol sensitive R3/4 provide the basis for polarization detection: should we not expect to see the opposite pattern?

This apparent paradox is resolved when one considers the non-linear response characteristics of photoreceptors. We assume that the probability of a photon being detected by a photoreceptor is a cosine function of its AoP relative to the orientation of the microvilli (Eqn 3). However, within its dynamic range, a photoreceptor responds logarithmically as a function of photon catch (Eqn 4). This has the effect of compressing the peaks and deepening the troughs of the cosine function. Thus, relative to un-pol light, the decrement in response elicited by polarized light orthogonal to the photoreceptor's tuning is greater in magnitude than the increment elicited by a perfectly aligned AoP (Fig. 6). Thus, the 'polarization distance' (Bernard and Wehner, 1977; How and Marshall, 2013) between V-pol and un-pol light is greater than that between H-pol and un-pol light. Therefore, a monopolatic detector composed of

photoreceptors that respond maximally to H-pol light is actually optimized for detecting V-pol light. A similar point was recently made by Belušič et al. (2017) with respect to the monopolatic eye of the corn borer moth.

Polarization perception depends on visual modality

Kinoshita et al. (2011) convincingly demonstrated that in a binary choice paradigm, foraging *P. xuthus* behaved as though they perceived equiluminant light of different AoPs to differ in brightness. Strikingly, this effect was in the opposite direction to that found in the present study: in the foraging task, V-pol light was perceived as brighter than un-pol light, which was in turn subjectively brighter than H-pol light. Therefore, when we presented a V-pol stripe against an objectively dimmer background, the stripe must have appeared substantially brighter than the background to the visual system that governs the foraging behaviour employed in Kinoshita et al.'s (2011) experiment, which we might term 'object vision'. However, in this situation, the motion vision system appears to detect no contrast (Fig. 2B).

This situation is puzzling, and difficult to reconcile with our conscious visual experience as humans. However, the observation is less surprising when one considers that flies (Yamaguchi et al., 2008) and bees (Kaiser and Liske, 1974) detect motion in a colour-blind manner, despite having the ability to discriminate colours. Together with these observations, our present finding further supports the view that vision is not a single, unified sense, but rather a collection of subsystems taking input from potentially dissimilar collections of photoreceptors and processing it through different neural circuitry, to serve distinct functions. Therefore, it is perhaps inappropriate to talk about an animals 'polarization vision' (or indeed 'colour vision' or 'brightness vision') in general; rather, these phenomena can only be understood with reference to a particular behavioural context.

Fig. 6. Monopolatic detectors and polarization distance. Response of an R3/4 photoreceptor in our model to light of varying AoP. The response to 45 deg polarization is identical to that of un-pol light; the two are indistinguishable (Eqn 3, Fig. 3A). Because of the photoreceptor's non-linear properties, the difference in responses elicited by un-pol (or diagonally polarized) and V-pol light (red bar) is larger than that between H-pol and un-pol (blue bar). The y-axis can thus be seen as a one-dimensional 'polarization space' in which V-pol (red circle) is further from un-pol than is H-pol (blue circle).

Functional significance: a bug or a feature?

An obvious question prompted by this study is what ecological purpose, if any, polarization-sensitive motion vision serves in *P. xuthus*. In our previous study, we took the view that chromatic motion vision likely offers no adaptive benefit in itself (Stewart

et al., 2015). Rather, we argued, the spectrally diverse set of photoreceptors evolved to improve colour vision for some other purpose (e.g. foraging or mating), and the motion vision system simply had to accommodate them. One could take a similar view of polarization sensitivity in motion vision, though in this case it is even less clear what the primary function of polarization-sensitive photoreceptors is.

The stimulus we used – chosen simply because it provided the most reliable behavioural response in our original study – perhaps complicates this question. The long, narrow stripe we presented could be viewed as a large-field stimulus suitable for estimating one's own motion by integrating optic flow signals across the retina. For instance, the butterfly could see the stripe as a horizon, and be attempting to compensate for a perceived perturbation to its pitch orientation. In contrast, it could see the stripe as a small-field target to be tracked against a static background. These functions are served by different neurons at the level of the lobula complex, in flies at least (Borst and Haag, 2002). However, as we hypothesize that polarization contrast affects local motion detection at the earlier processing stage of the lamina, we would expect polarization effects to be common to all downstream motion-processing circuits.

We speculate that polarization-sensitive motion vision could actually be adaptive in the context of small-field target detection. This appears to be the case in fiddler crabs, which – like *P. xuthus* – have polarization sensitivity throughout their eyes. Looming unpolarized objects against a polarized background elicit escape behaviours in these animals, indicating that they perceive these stimuli as predators and/or hostile conspecifics (How et al., 2014, 2015). The main predators of *Papilio* are birds, which would tend to appear as dark objects against a bright sky. Atmospheric scattering causes light to be polarized in a concentric pattern around the sun; this is the basis of the 'celestial compass' used by other insects for navigation. When the sun is at the zenith, therefore, the entire sky is horizontally polarized (to varying degree). For a butterfly active around noon in summer (as *Papilio* are), the monopolatic scheme we have described would enhance the contrast of a moving dark, relatively unpolarized bird against a bright, roughly H-pol sky. Of course, whether this hypothesized enhancement is sufficient to offer an ecologically relevant advantage remains to be tested behaviourally.

Competing interests
The authors declare no competing or financial interests.

Author contributions
Conceptualization: F.J.S., M.K., K.A.; Methodology: F.J.S.; Software: F.J.S.; Investigation: F.J.S.; Writing - original draft: F.J.S.; Writing - review & editing: M.K., K.A.

Supplementary information
Supplementary information available online at
http://jeb.biologists.org/lookup/doi/10.1242/jeb.191957.supplemental

References

Arikawa, K. and Uchiyama, H. (1996). Red receptors dominate the proximal tier of the retina in the butterfly *Papilio xuthus*. *J. Comp. Physiol. A* **178**, 55-61.

Arikawa, K., Mizuno, S., Scholten, D. G. W., Kinoshita, M., Seki, T., Kitamoto, J. and Stavenga, D. G. (1999). An ultraviolet absorbing pigment causes a narrow-band violet receptor and a single-peaked green receptor in the eye of the butterfly *Papilio*. *Vision Res.* **39**, 1-8.

Awata, H., Wakakuwa, M. and Arikawa, K. (2009). Evolution of color vision in pierid butterflies: blue opsin duplication, ommatidial heterogeneity and eye regionalization in *Colias erate*. *J. Comp. Physiol. A* **195**, 401-408.

Awata, H., Matsushita, A., Wakakuwa, M. and Arikawa, K. (2010). Eyes with basic dorsal and specific ventral regions in the glacial Apollo, *Parnassius glacialis* (Papilionidae). *J. Exp. Biol.* **213**, 4023-4029.

Bandai, K., Arikawa, K. and Eguchi, E. (1992). Localization of spectral receptors in the ommatidium of butterfly compound eye determined by polarization sensitivity. *J. Comp. Physiol. A.* **171**, 289-297.

Belušič, G., Šporar, K. and Meglič, A. (2017). Extreme polarisation sensitivity in the retina of the corn borer moth *Ostrinia*. *J. Exp. Biol.* **220**, 2047-2056.

Bernard, G. D. and Wehner, R. (1977). Functional similarities between polarization vision and color vision. *Vision Res.* **17**, 1019-1028.

Borst, A. and Haag, J. (2002). Neural networks in the cockpit of the fly. *J. Comp. Physiol. A* **188**, 419-437.

Foster, J. J., Temple, S. E., How, M. J., Daly, I. M., Sharkey, C. R., Wilby, D. and Roberts, N. W. (2018). Polarisation vision: overcoming challenges of working with a property of light we barely see. *Sci. Nat.* **105**, 27.

How, M. J. and Marshall, N. J. (2014). Polarization distance: a framework for modelling object detection by polarization vision systems. *Proc. R. Soc. B Biol. Sci.* **281**, 20131632.

How, M. J., Christy, J., Roberts, N. W. and Marshall, N. J. (2014). Null point of discrimination in crustacean polarisation vision. *J. Exp. Biol.* **217**, 2462-2467.

How, M. J., Christy, J. H., Temple, S. E., Hemmi, J. M., Marshall, N. J. and Roberts, N. W. (2015). Target detection is enhanced by polarization vision in a fiddler crab. *Curr. Biol.* **25**, 3069-3073.

Joesch, M., Schnell, B., Raghu, S. V., Reiff, D. F. and Borst, A. (2010). ON and OFF pathways in *Drosophila* motion vision. *Nature* **468**, 300-304.

Kaiser, W. and Liske, E. (1974). Die optomotorischen Reaktionen von fixiert fliegenden Bienen bei Reizung mit Spektrallichtern. *J. Comp. Physiol.* **89**, 391-408.

Kawasaki, M., Kinoshita, M., Weckström, M. and Arikawa, K. (2015). Difference in dynamic properties of photoreceptors in a butterfly, *Papilio xuthus*: possible segregation of motion and color processing. *J Comp Physiol A Neuroethol Sens Neural Behav Physiol.* **201**, 1115-1123.

Kelber, A. (1999). Why 'false' colours are seen by butterflies. *Nature* **402**, 251-251.

Kelber, A., Thunell, C. and Arikawa, K. (2001). Polarisation-dependent colour vision in *Papilio* butterflies. *J. Exp. Biol.* **204**, 2469-2480.

Kinoshita, M. and Arikawa, K. (2014). Color and polarization vision in foraging *Papilio*. *J. Comp. Physiol. A* **200**, 513-526.

Kinoshita, M., Yamazato, K. and Arikawa, K. (2011). Polarization-based brightness discrimination in the foraging butterfly, *Papilio xuthus*. *Philos. Trans. R. Soc. B Biol. Sci.* **366**, 688-696.

Kitamoto, J., Sakamoto, K., Ozaki, K., Mishina, Y. and Arikawa, K. (1998). Two visual pigments in a single photoreceptor cell: identification and histological localization of three mRNAs encoding visual pigment opsins in the retina of the butterfly *Papilio xuthus*. *J. Exp. Biol.* **201**, 1255-1261.

Koshitaka, H., Kinoshita, M., Vorobyev, M. and Arikawa, K. (2008). Tetrachromacy in a butterfly that has eight varieties of spectral receptors. *Proc. R. Soc. B Biol. Sci.* **275**, 947-954.

Labhart, T. (2016). Can invertebrates see the e-vector of polarization as a separate modality of light? *J. Exp. Biol.* **219**, 3844-3856.

Naka, K. I. and Rushton, W. A. H. (1966a). S-potentials from luminosity units in the retina of fish (Cyprinidae). *J. Physiol.* **185**, 587-599.

Naka, K. I. and Rushton, W. A. H. (1966b). S-potentials from colour units in the retina of fish (Cyprinidae). *J. Physiol.* **185**, 536-555.

Stavenga, D. G., Kinoshita, M., Yang, E.-C. and Arikawa, K. (2001). Retinal regionalization and heterogeneity of butterfly eyes. *Naturwissenschaften* **88**, 477-481.

Stewart, F. J., Kinoshita, M. and Arikawa, K. (2015). The butterfly *Papilio xuthus* detects visual motion using chromatic contrast. *Biol. Lett.* **11**, 20150687.

Stewart, F. J., Kinoshita, M. and Arikawa, K. (2017). A novel display system reveals anisotropic polarization perception in the motion vision of the butterfly *Papilio xuthus*. *Integr. Comp. Biol.* **57**, 1130-1138.

Wässle, H. (2004). Parallel processing in the mammalian retina. *Nat. Rev. Neurosci.* **5**, 747-757.

Yamaguchi, S., Wolf, R., Desplan, C. and Heisenberg, M. (2008). Motion vision is independent of color in *Drosophila*. *Proc. Natl. Acad. Sci. USA* **105**, 4910-4915.